Assignment of Proton Resonances, Identification of Secondary Structural Elements, and Analysis of Backbone Chemical Shifts for the C102T Variant of Yeast Iso-1-cytochrome *c* and Horse Cytochrome *c*†

Yuan Gao,‡ Jonathan Boyd,§ Robert J. P. Williams,‡ and Gary J. Pielak*,∥

Inorganic Chemistry Laboratory, University of Oxford, Oxford OX1 3QR, U.K., Department of Biochemistry, University of Oxford, Oxford OX1 3QU, U.K., Department of Chemistry and the Program in Molecular Biology and Biotechnology, University of North Carolina at Chapel Hill, Chapel Hill, North Carolina 27599-3290

Received November 14, 1989; Revised Manuscript Received January 19, 1990

ABSTRACT: Resonance assignments for the main-chain, side-chain, exchangeable side chain, and heme protons of the C102T variant of *Saccharomyces cerevisiae* iso-1-cytochrome *c* in both oxidation states (with the exception of Gly-83) are reported. (We have also independently assigned horse cytochrome *c*.) Some additional assignments for the horse protein extend those of Wand and co-workers [Wand, A. J., Di Stefano, D. L., Feng, Y., Roder, H., & Englander, S. W. (1989) *Biochemistry 28*, 186–194; Feng, Y., Roder, H., Englander, S. W., Wand, A. J., & Di Stefano, D. L. (1989) *Biochemistry 28*, 195–203]. Qualitative interpretation of nuclear Overhauser enhancement data allows the secondary structure of these two proteins to be described relative to crystal structures. Comparison of the chemical shift of the backbone protons of the C102T variant and horse protein reveals significant differences resulting from amino acid substitution at positions 56 and 57 and further substitutions between residue 60 and residue 69. Although the overall folding of yeast iso-1-cytochrome *c* and horse cytochrome *c* is very similar, there can be large differences in chemical shift for structurally equivalent residues. Chemical shift differences of amide protons (and to a lesser extent α protons) represent minute changes in hydrogen bonding. Therefore, great care must be taken in the use of differences in chemical shift as evidence for structural changes even between highly homologous proteins.

The cytochrome *c* from horse has historically been the most studied member of this important class of electron-transfer proteins. Recently, however, many studies of structure and function have utilized iso-1-cytochrome *c* from the yeast *Saccharomyces cerevisiae*. Reasons for the keen interest in the yeast system include the ease with which yeast may be genetically altered and the subsequent ability to express the altered proteins. One drawback to the use of iso-1-cytochrome *c* as an experimental system is the presence of a free sulfhydryl group in the protein sequence which proves to be problematical (because of its redox properties) in function studies. This residue has therefore been changed to Thr (Cutler et al., 1987). The resulting C102T protein is well-behaved with respect to oxidation and reduction and it is the object of this paper.

In the past several years many mutants of iso-1-cytochrome *c* have been produced by using either site-directed mutagenesis or classical genetic methods. Kinetic studies have included measurement of the effects of amino acid substitutions on the first-order (Liang et al., 1987, 1988; Hazzard et al., 1988) and steady-state (Pielak et al., 1985; Cutler et al., 1987, 1989) rates of electron transfer, in in vitro systems involving physiological redox partners. Thermodynamic studies have included measuring effects on reduction potential (Pielak et al., 1985; Cutler et al., 1987, 1989; Sorrell & Martin, 1989), on the alkaline transition (Pearce et al., 1989), and on the binding of exogenous ligands (Y. Gao, G. J. Pielak, and R. J. P. Williams, unpublished results).

To understand fully the causes of functional changes brought about by amino acid substitutions, it is necessary to know the structure of the mutated cytochromes *c*. To this end, the techniques of circular dichroism (Pielak et al., 1986), X-ray crystallography (Louie et al., 1988a,b), and nuclear magnetic resonance (NMR)[1] (Pielak et al., 1988a,b) have been applied to yeast iso-1-cytochrome *c*. NMR and crystallography can be used to examine structure at the molecular level. These two techniques often yield complementary information. While crystallography usually gives structures of higher resolution than NMR, it gives less direct information about the dynamics of protein structure and chemical properties. NMR may well provide information about hydrogen-bond strengths, too, as we shall demonstrate here.

Recently, NMR has been used to assign the proton resonances in both the reduced and oxidized forms of the horse protein. The most extensive data are given by Wand et al. (1989) and Feng et al. (1989), who cite a complete set of references to earlier work. Assignments for the main chain of the tuna and horse proteins have been reported and compared to each other (Gao et al., 1989). In this paper we report assignments for the oxidized and reduced forms of the C102T variant and some additional assignments for the horse protein (supplementary material), which we shall need in our comparison of redox properties.

Yeast iso-1-cytochrome *c* bears an N-terminal extension of five amino acids, with respect to higher eukaryotic cytochromes *c*. In this paper the numbering system for higher eukaryotic cytochromes *c* is used, resulting in negative numbers for res-

† This work was supported by grants from the Medical Research Council, the Science and Engineering Research Council, and the Royal Society.

* Address correspondence to this author.
‡ Inorganic Chemistry Laboratory, University of Oxford.
§ Department of Biochemistry, University of Oxford.
∥ University of North Carolina.

[1] Abbreviations: COSY, correlated spectroscopy; DRCT, double-relayed coherence transfer, 2-D, two-dimensional; NMR, nuclear magnetic resonance; NOE, nuclear Overhauser effect; NOESY, NOE-correlated spectroscopy; ppm, parts per million; pre-TOCSY, pre total coherence spectroscopy; RCT, relayed coherence transfer.

0006-2960/90/0429-6994$02.50/0

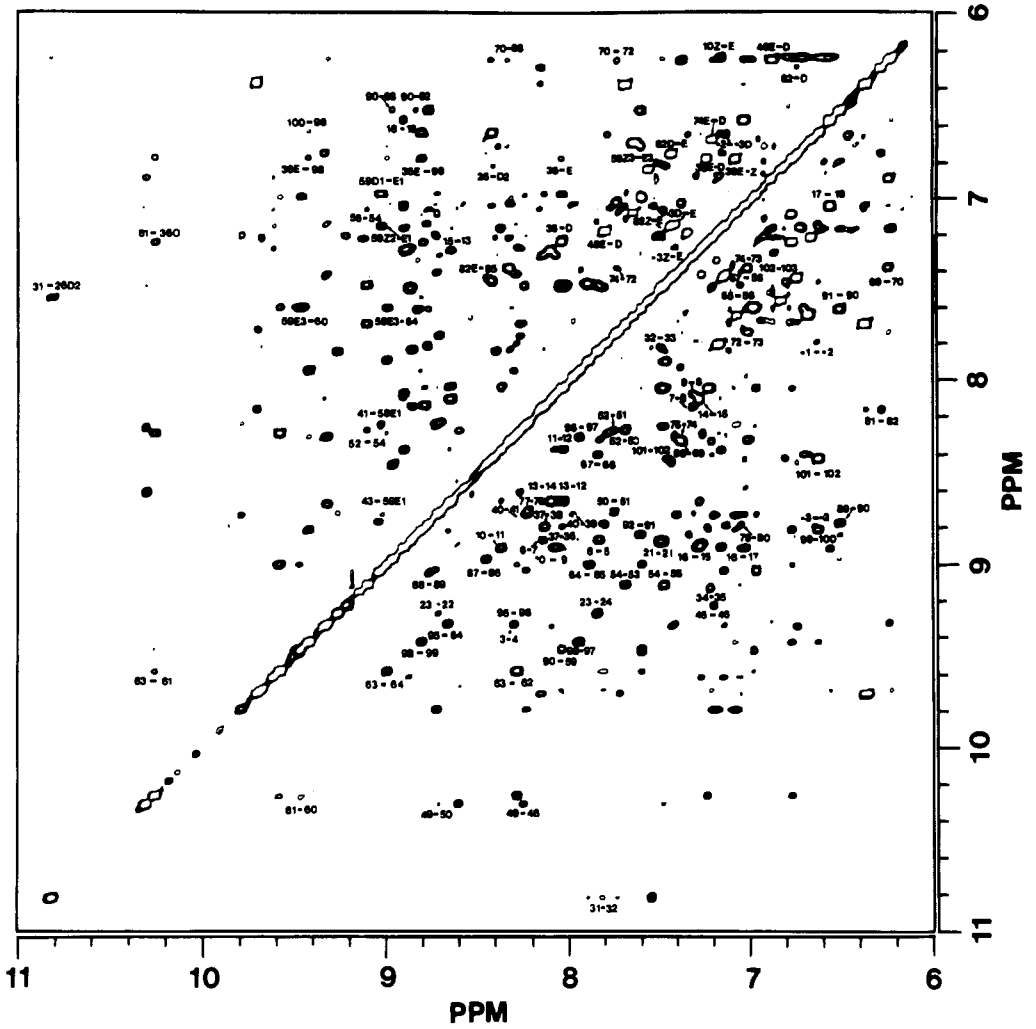

FIGURE 1: Amide and aromatic region of the NOESY spectrum of the C102T variant of yeast iso-1-ferrocytochrome c. Connectivities involving pairs of neighboring amide protons are labeled in the region below the diagonal. Long-range amide connectivities and amide–aromatic connectivities are labeled in the region above the diagonal. In this and the following figures A, B, G, D, E, H, and Z refer to α, β, γ, δ, ϵ, η, and ζ, respectively.

idues comprising the extension.

Materials and Methods

Preparation and purification of the C102T variant used in this study has been previously described (Cutler et al., 1987). Horse heart cytochrome c was purchased from Sigma (type VI) and purified before use by gradient elution ion-exchange chromatography on Whatman CG-50. NMR data were collected on a home-built 500-MHz spectrometer and processed by using a GE/Nicolet 1280 computer and acquisition software as described in Pielak et al. (1988a,b). Samples were prepared for NMR spectroscopy as described by Pielak et al. (1988a). All NMR data were collected at 300 K in 90% H_2O/10% D_2O. Two-dimensional (2-D) correlated (COSY), relayed coherence transfer (RCT) (τ = 15 ms) spectra and 2-D nuclear Overhauser enhancement (NOESY) spectra (mixing time of 133 ms) were collected by using the acquisition method of States et al. (1982). Double-relayed COSY (DRCT) spectra were obtained by the insertion of an additional coherence transfer step ($-\tau-180°-\tau-90°$; τ = 15 ms) after the traditional sequence for RCT. Pre total correlation spectroscopy (pre-TOCSY) COSY and NOESY spectra were obtained as described by Otting and Wüthrich (1987). The transmitter offset was set on H_2O and its resonance was eliminated by presaturation for 1 s. IUB–IUPAC nomenclature is used in identifying amino acid protons, except for the hydroxy group of Thr which is referred to as OH. 1,4-Dioxane was used as an internal chemical shift reference at 3.74 parts per million (ppm) to external 2,2-trimethyl-2-silapentane-5-sulfonate. The assignments reported here are reliable to within 0.01 ppm.

Results

In this paper we have chosen to present spectra of the reduced C102T variant. Spectra of the oxidized C102T variant and of the oxidized horse protein (available as supplementary material) are of equal quality.

NOESY spectra were examined in the amide region (Figure 1) to obtain sequential stretches of amide proton connectivities. The procedures used are largely those described by Wüthrich (1986).

The chemical shifts of the individual sequential amide protons defined above were used to locate the amide–α cross peaks in the fingerprint region of the COSY spectrum (Figure 2). RCT (data not shown) and DRCT spectra (Figure 3) were then used to obtain β and γ assignments for individual amide protons. For many residues this allowed assignment of entire spin systems. Use was also made of α–β, α–γ, and α–δ connectivities from COSY, RCT, and DRCT (Figures 4 and 5) spectra. Comparison of these data with the amino acid sequence allowed the range of sequential assignments to be placed within the context of the deduced protein sequence (Smith et al., 1979). As discussed previously (Wand & Englander 1985; Pielak et al., 1988a,b), the ability to compare

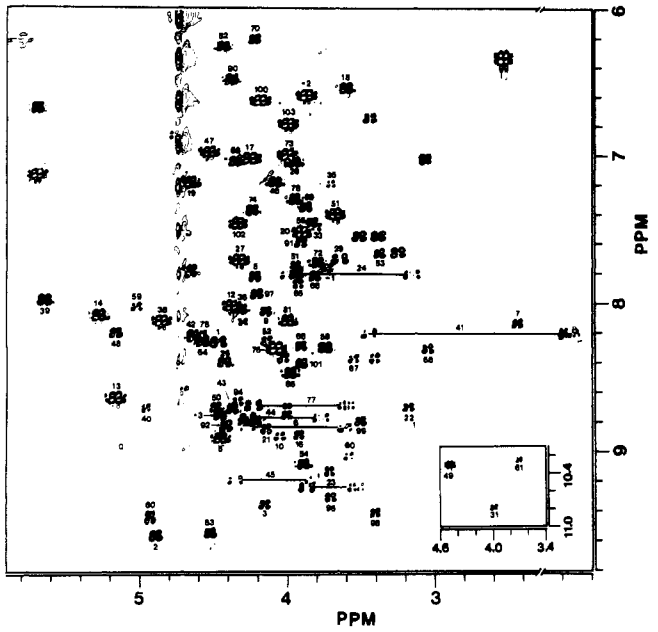

FIGURE 2: Fingerprint region of the COSY spectrum of the C102T variant of yeast iso-1-ferrocytochrome *c*. Horizontal lines connect the α proton resonances of Gly residues.

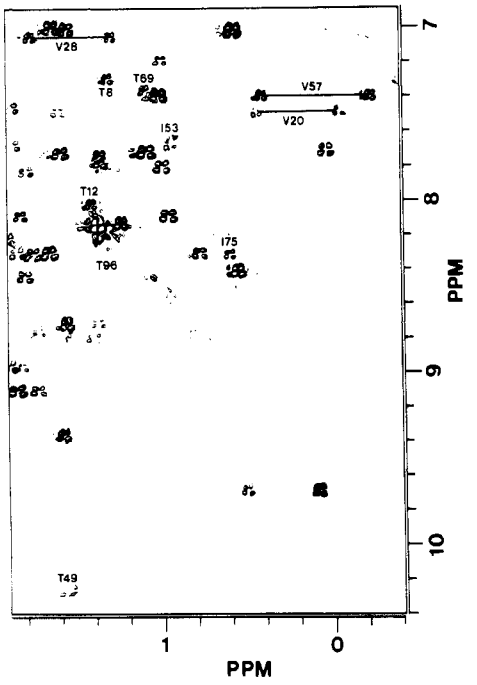

FIGURE 3: DRCT COSY spectrum of the C102T variant of yeast iso-1-ferrocytochrome *c*. Amide–γ2 DRCT peaks of two Ile and amide–γ DRCT peaks of three Val and five Thr residues are labeled. Horizontal lines connect the γ proton resonances of Val residues.

data from two very similar proteins greatly aided the assignment procedure. Heme resonances were assigned and are in excellent agreement with those of Senn et al. (1983). Proton assignments for the reduced and oxidized forms of the C102T variant are given in Table I. Tables containing proton assignments for the horse protein are available as supplementary material.

As can be seen from Table II, sequential amide–amide connectivities (Figure 1) of greater than two residues were observed for positions −3 to −1 in the C102T variant and residues 1–17, 22–24, 31–42, 47–57, 59–69, 72–74, 79–82, 88–91, and 93 to the C-terminus in either or both proteins. There are several trivial reasons for gaps in the amide–amide connectivities. Gaps at positions 24–25 (C102T), 43–44 (horse protein), 70–71, and 75–76 are due to the presence of Pro residues. Possible amide–amide connectivities at positions 43, 65, 85, and 87 in the C102T protein, positions 4, 10, 19, 21, 27, 46, 96, and 98 in the horse protein, positions and 41, 67, and 92 in both proteins cannot be observed because of nearly degenerate (within 0.10 ppm) amide proton chemical shifts at positions *i* and *i*+1. Possible connectivities involving positions 82 (C102T), 83, and 84 are unobservable because the amide proton of Gly-84 (and Gly-83 in C102T) remains unassigned. A table similar to Table II giving connectivities for the oxidized C102T variant and the horse protein is available as supplementary material.

With α and side-chain proton assignments in hand, NOESY spectra were reexamined for amide–α, β–amide, and longer range sequential NOEs (Table II). This strategy serves as a useful check on main-chain assignments based on only amide–amide connectivities. Representative samples of annotated portions of the NOESY spectra are shown in Figures 6 and 7. Annotated portions of the NOESY spectra showing amide–amide connectivities for residues 50–57, 59–70, and 72–75 are available as supplementary material. Several cases where longer range backbone NOEs are not observed in both proteins (Table II) are most likely due to degeneracy in chemical shifts as described above. For instance, an α–amide (*i*,*i*+3) connectivity would be impossible to observe for either ferrocytochrome *c* at position 90 because the chemical shift for the α proton is the same as that for α (*i*+3) (Table I and supplementary material).

Identification of Helical Regions. Although short amide–amide distances are necessary for identification of helical structure, they are not sufficient (Wüthrich, 1986). A better indicator of α-helical structure is the observation of backbone (*i*,*i*+3) NOEs. As can be seen from data in Table II, α–β-(*i*,*i*+3) connectivities are observed for residues 6–9, 11, 80, 93, and 95–100. α–Amide (*i*,*i*+3) connectivities are observed for residues 3–8, 10, 14, 15, 50, 51, 88, 89, 91–93, and 96–100. The gap at position 95 is due to the degeneracy of the chemical shifts of the amide protons of positions 95 and 98. Several β–amide (*i*,*i*+3) and α–amide (*i*,*i*+4) connectivities are also observed in these regions. α–Amide (*i*,*i*+2) cross peaks are indicative of 3_{10} helical elements (Wüthrich, 1986). A run of four of this type of NOE is observed for residues 13–16. It is interesting to note that a string of amide–amide (*i*,*i*+2) connectivities is also observed between positions 60 and 64.

Discussion

An extensive set of assignments for horse ferrocytochrome *c* has recently been published (Feng et al., 1989). The data in Tables I and II and the supplementary material confirm and extend these results. The chemical shifts for the same protons from our assignment of the horse protein are about 0.05–0.10 ppm smaller than those reported by Feng et al. (1989). This systematic difference may be due to the minor differences in temperature, ionic strength, buffer, and spectral referencing between the two studies. The results of the two studies are in excellent agreement.

The published crystal structure of the horse protein (Dickerson et al., 1970) is at comparatively low resolution with respect to the crystal structures of yeast iso-1-cytochrome *c* (Louie et al., 1988a) and rice (Ochi et al., 1983), bonito (Tanaka et al., 1975; Matsuura et al., 1979), and tuna cytochromes *c* (Takano & Dickerson, 1981a,b). Louie et al. (1988a) used least-squares structural overlap analysis to compare the main-chain conformation of yeast iso-1-cytochrome *c* (reduced) and rice (oxidized) and tuna (oxidized and

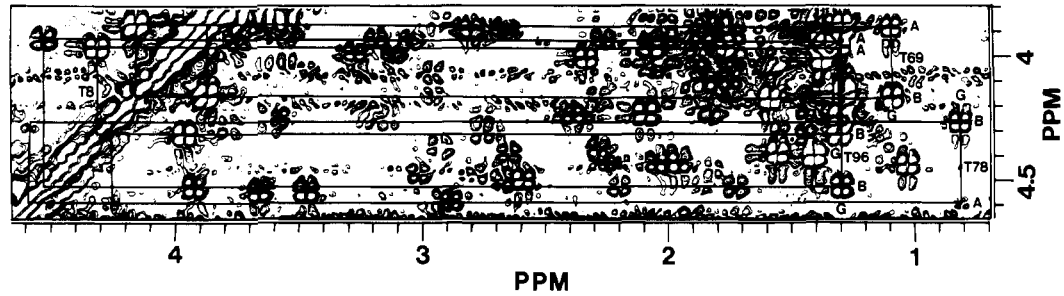

FIGURE 4: DRCT COSY spectrum of the C102T variant of yeast iso-1-ferrocytochrome *c*. β–γ COSY and α–γ RCT peaks of four Thr residues are labeled. Vertical lines are shown connecting α and β with γ protons; vertical lines connect γ to α and β proton resonances.

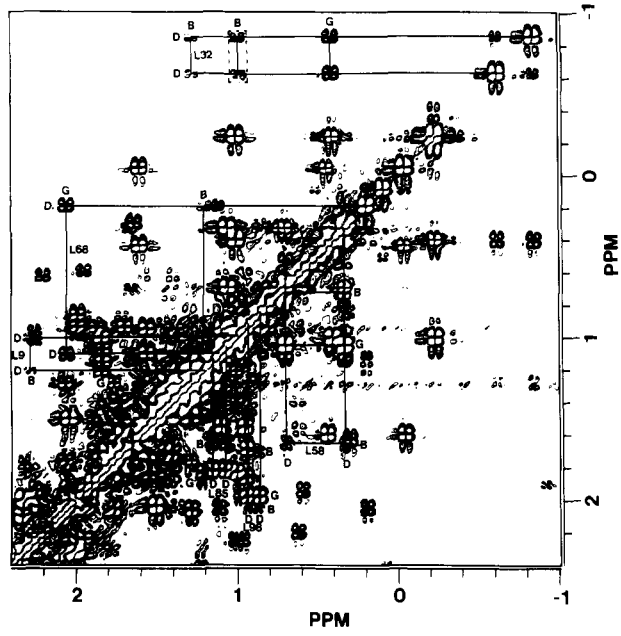

FIGURE 5: DRCT COSY spectrum of the C102T variant of yeast iso-1-ferrocytochrome *c*. β–δ RCT and β–γ COSY peaks of six Leu residues are labeled. Horizontal and vertical lines are used to define the spin system of individual residues.

reduced) cytochromes *c*. The root mean square difference ranges from 0.42 to 0.63 Å. Although yeast iso-1-cytochrome *c* and horse cytochrome *c* were not compared, it is unlikely that the difference between the C102T variant and horse heart cytochrome *c* differs significantly from the above values. What emerges clearly from examination of all these structures is that eukaryotic cytochromes *c* are composed of five helical elements and four type II β turns. The NOE data presented in Table II are fully consistent with this description, and we consider sections of the sequence in turn.

Extension Present at the N-Terminus of Fungal and Plant Cytochromes c. The observation of amide–amide, amide–α, and amide–β connectivities for this region of the C102T variant (Table II) is evidence that this region does possess inherent structure in solution. Since $(i,i+3)$ connectivities are not observed, this structure appears not to be helical. In the X-ray crystal structure of both the iso-1-cytochrome *c* and rice (which has an extension of eight residues) cytochrome *c*, this region is described as having extended structure (Louie et al., 1988a; Ochi et al., 1983).

N- and C-Terminal Helices. The observation of consecutive α–amide $(i,i+3)$, β–amide $(i,i+3)$, α–β $(i,i+3)$, and α–amide $(i,i+4)$ strongly supports the conclusion that residues 3–13 form an α helix. The observation of $(i,i+2)$ connectivities suggests some distortion in the central and end region of the helix. This distortion has been previously noted for tuna ferricytochrome *c* by Williams (1986). There also is a turn of a helical nature between residues 13 and 18. The region from 14 to 18 contains the two thioether linkages to the heme (Cys-14 and -17) and the histidine ligand to the iron (His-18). Turning to the C-terminal helix, 10 α–amide $(i,i+3)$ and α–β $(i,i+3)$ connectivities are observed within the sequence of residues 88–99. Although six $(i,i+2)$ connectivities are observed between residue 88 and the C-terminus, none are consecutive. This suggests the C-terminus forms a more regular α helix than does the N-terminus. The extent of the N- and C-terminal α helices as described by X-ray crystallography includes residues 5–14 and 88 to the C-terminus, respectively.

50s, 60s and 70s Helices. Two $(i,i+4)$ and five $(i,i+3)$ NOEs are observed between residues 49 and 54 (Table II), suggesting an α-helical motif. However, the observation of

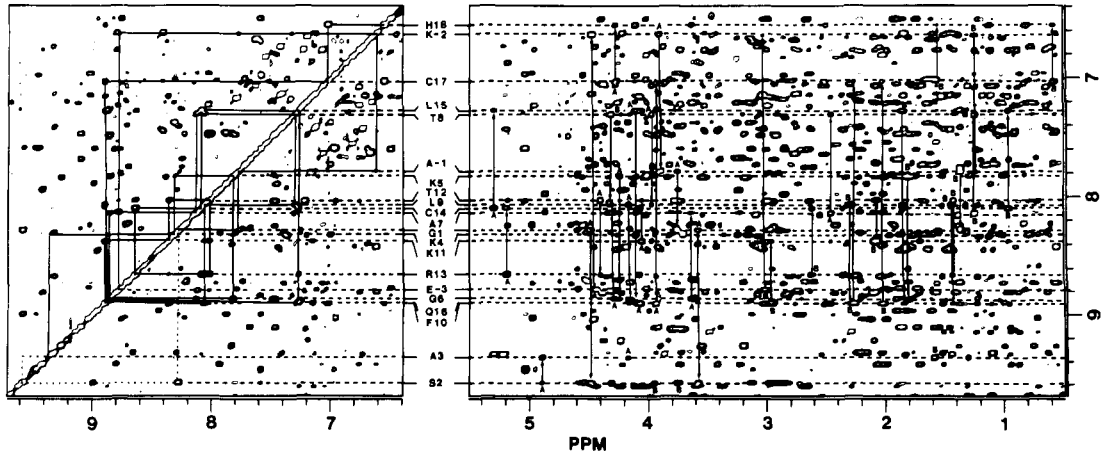

FIGURE 6: NOESY spectrum of the C102T variant of yeast iso-1-ferrocytochrome *c*. Sequential amide–amide connectivities for residues 3–18 are indicated with solid horizontal and vertical lines on the left. Dashed horizontal lines are drawn at the chemical shift of amide protons. Sequential α–amide and β–amide connectivities are indicated by vertical lines on the right.

Table I: Proton Assignments for Yeast C102T Iso-1-cytochrome *c* at 300 K[a]

residue	amide	α^b	α^b	β^b	β^b	others[b]	residue	amide	α^b	α^b	β^b	β^b	others[b]
Phe--3	8.77	4.48		2.73	3.01	57.14, ε 7.42, ζ 7.26	Pro-30		3.80		−0.25	1.37	γ −0.49, γ −0.72
	8.68	4.33		2.62	2.87	δ 6.96, ε 7.21							δ −1.45, δ −5.44
						ζ 7.08	Asn-31	10.82	4.02		1.98	2.17	δ2 7.46, δ2 7.88
Lys--2	6.63	3.91		1.24	1.50			11.76	5.88		2.59	2.98	δ2 8.13, δ2 8.81
	6.57	3.83		1.27	1.40	γ 1.14	Leu-32	7.80	3.97		1.00	1.29	γ 0.42, δ −0.84
Ala--1	7.78	3.74		1.37									δ −0.62
	7.69	3.63		1.26				9.52	4.78		2.41	2.05	
Gly-1	8.28	3.58	4.50				His-33	7.48	3.84		2.92	3.04	δ2 7.30, ε1 8.39
	8.11	3.40	4.35					8.17	4.15		3.28	3.37	
Ser-2	9.58	4.90		3.76	3.95		Gly-34	9.12	3.73	3.82			
	9.40	4.72		3.40	3.62			9.27	3.71	3.82			
Ala-3	9.36	4.18		1.60			Ile-35	7.22	3.73		1.64		γ1 0.87, γ1 1.23
	9.23	4.00		1.50									γ2 0.32, δ 0.73
Lys-4	8.31	4.31						7.17	3.68		1.66		γ1 1.05, γ1 0.60
	8.16												γ2 0.12, δ 0.50
Lys-5	7.75	4.24		1.88	2.02		Phe-36	8.02	4.35		2.99	3.77	δ 7.22, ε 6.77
	7.69	4.09		1.72									ζ 7.07
Gly-6	8.90	3.63	4.30					8.02	4.06		2.82	2.95	δ 7.01, ε 6.41
	8.68	3.28	4.00										ζ 6.45
Ala-7	8.13	2.46		1.23			Gly-37	8.78	3.80	4.27			
	8.01	2.40		1.23				8.83	3.65	4.25			
Thr-8	7.30	3.97		4.32		γ 1.32	Arg-38	8.12	4.87		2.02	2.09	γ 1.88, γ 2.23
	7.21	3.92		4.17		γ 1.22							δ 3.21, δ 3.28
Leu-9	8.07	4.17		1.45	2.29	γ 1.85, δ 1.02							ε 7.66, η 9.12
						δ 1.22		7.95	4.67		1.84	2.00	δ 3.20, δ 3.70
	7.82	3.80		1.83		γ 1.49, δ 0.56							ε 7.28
						δ 0.80	His-39	7.97	5.66		2.85	3.02	δ2 7.02, ε1 8.57
Phe-10	8.90	4.07		2.97	3.02	δ 7.15, δ 7.15		8.20	5.25		2.89	3.02	δ2 7.01, ε1 8.58
						ε 6.85, ε 6.20	Ser-40	8.72	4.98		2.36	2.42	
						ζ 6.21		8.68	4.52		3.62		
	8.62	3.51		2.75	2.99	δ 7.82, δ 7.16	Gly-41	8.23	1.38	3.47			
						ε 7.22, ε 7.22		8.95	1.09	3.10			
						ζ 8.60	Gln-42	8.22	4.67		1.94		γ 2.08, γ 2.43
Lys-11	8.37	4.04		1.71[c]	2.08[c]								ε2 6.82, ε2 7.54
	8.44	4.33		2.18				7.85	4.46		1.68	2.43	γ 2.13, γ 2.19
Thr-12	8.03	4.40		4.40		γ 1.43							ε2 6.78, ε2 7.31
	7.88	4.35		4.21		γ 1.33	Ala-43	8.72	4.38		1.57		
Arg-13	8.64	5.20		2.35	2.62	γ 1.95, γ 2.25		8.12	4.32		1.43		
						δ 3.42, δ 3.54	Glu-44	8.81	4.23		2.11	2.43	γ 2.36
						ε 7.55		8.83	4.12		2.07	2.40	γ 2.33
	8.19	4.57		1.00			Gly-45	9.22	3.83	4.38			
Cys-14	8.08	5.30		0.97	1.84			9.07	3.70	4.27			
	7.92						Tyr-46	7.18	4.10		1.00	2.21	δ 6.22, δ 4.45
Leu-15	7.27	4.05		1.86	1.38	γ 1.56, δ 1.10							ε 6.86, ε, 7.40
	8.04	6.07		2.18	2.53	γ 2.35, δ 1.48							η 9.31
Gln-16	8.90	3.93		2.02	2.27[c]	γ 2.53, γ 2.77		6.96	3.67		0.60	1.63	δ 5.68, δ 3.81
						ε2 7.05, ε2 7.63							ε 5.07, ε 5.48
	9.99	4.68		2.67	2.86	γ 2.98, ε2 6.90	Ser-47	6.96	4.55		3.48	3.67	
						ε2 7.60		6.46	4.04		2.99	3.16	
Cys-17	7.03	4.28		0.58	1.57		Tyr-48	8.23	5.18		2.94	3.77	δ 7.45, δ 8.02
	9.74	6.11		3.03	2.47								ε 7.06, ε 7.20
His-18	6.54	3.63		0.81	1.12[c]	δ2 0.11, ε1 0.52							η 9.78
	11.02	8.87		8.77	14.96	δ2 −25.85, ε1 24.24		7.72	4.08		2.47	3.24	δ 6.95
Thr-19	7.19	4.67		4.45		γ 1.10	Thr-49	10.30	4.51		4.73		γ 1.81, OH 8.60
	10.15	6.31		5.48		γ 2.16, OH 8.81		9.63	4.18		4.62		γ 1.48, OH 8.19
Val-20	7.48[c]	3.92		1.62		γ −0.03, γ 0.45	Asp-50	8.70	4.52		2.62	2.70	
	8.53	4.92		2.18		γ 0.90, γ 1.05		8.63	4.37		2.57	2.67	
Glu-21	8.87	4.15		1.87	1.92		Ala-51	7.74[c]	3.97		1.37		
	9.58	4.52		2.17	2.26			8.03	4.13		1.63		
Lys-22	8.71	3.21		0.52	1.38	γ 0.75, γ 1.00	Asn-52	8.27	4.15		2.96	3.13	
						δ 1.45, ε 2.86		8.35	4.62		2.92	3.19	δ2 7.08, δ2 7.39
	9.00	3.47			1.56		Ile-53	7.67	3.40		1.88		γ1 1.18, γ1 1.94
Gly-23	9.26	3.57	3.91										γ2 0.96, δ 1.10
	9.52	3.76	4.09					7.63	3.60		1.88		γ1 1.06, γ1 1.56
Gly-24	7.82	3.18	4.02										γ2 0.88, δ 0.89
	8.24	3.70	4.41				Lys-54	9.10	3.92		1.74	1.87	
Pro-25		4.18		2.04				9.04	3.97				
		4.52	2.17	2.35			Lys-55	7.46	3.84		1.90		
His-26	8.41	4.44		2.79	3.08	δ2 7.03, ε1 7.52		7.39	4.06		1.94		
	8.78	5.04		2.78	3.12	δ2 6.98, ε1 7.68	Asn-56	7.04	4.38		2.29	2.93	δ2 6.35, δ2 7.67
Lys-27	7.72	4.35		1.07	1.13			7.30	4.37		2.33	3.05	δ2 6.50, δ2 7.53
	8.32	4.68		1.78	2.45		Val-57	7.40	3.70		1.02		γ −0.22, γ 0.42
Val-28	7.05	3.98		2.08		γ 1.30, γ 1.77		7.28	4.09		1.35		γ 0.15, γ 0.36
	7.54	3.05		1.31		γ −0.40, γ 0.80	Leu-58	8.32	3.77		1.67	0.77	γ 1.08, δ 0.34
Gly-29	7.71	0.03	3.68										δ 0.71
	7.47	−0.49	−3.23					8.28	3.86		0.86	1.55	γ 1.02, δ 0.38
Pro-30		3.61		0.42	1.28								δ 0.63

Table I (Continued)

residue	amide	α^b	α^b	β^b	β^b	others[b]	residue	amide	α^b	α^b	β^b	β^b	others[b]
Trp-59	8.03	5.03		2.63	3.73	ϵ3 7.59, ζ3 6.69	Ala-81	8.15	4.02		1.38		
						η3 5.70, ζ2 7.14		8.26	5.18		1.33		
						δ1 6.97, ϵ1 9.02	Phe-82	6.26	4.45		0.61	2.04	δ 6.73, ϵ 7.42
	7.91	4.92		2.37	3.56	ϵ3 7.52, ζ3 6.69							ζ 7.14
						η3 6.47, ζ2 7.55		8.79	4.67				δ 6.18, ϵ 6.18
						δ1 6.85, ϵ1 8.93							ζ 5.87
Asp-60	9.47	4.97		3.13	2.83		Gly-83						
	9.92	4.79					Gly-84		3.03	4.26			
Glu-61	10.25	3.72		1.55	1.12				3.07	4.46			
	10.02	3.38		1.44	1.15		Leu-85	8.43	4.76		1.45		γ 1.84, δ 1.08
Asn-62	8.27	4.60		2.90	2.99	δ2 7.17, δ2 7.79							δ 1.18
	8.20	4.47		2.83	2.92	δ2 7.10, δ2 7.75		8.07	4.34		0.80	1.08	γ 0.90, δ 0.02
Asn-63	9.58	4.55		2.84	3.13	δ2 6.97, δ2 7.58							δ 0.38
	9.45	4.56		2.90	3.26	δ2 7.03, δ2 7.37	Lys-86	8.46	4.00		1.81	1.83	
Met-64	8.99	4.70		2.25	2.74	ϵ 1.24		8.33	3.90		1.70	1.80	
	8.78	4.30		1.73	2.21	γ 2.37, γ 3.55	Lys-87	8.96	4.48		1.83	1.91	
						ϵ 0.21		8.70	4.30		1.43	1.67	
Ser-65	7.88	3.95		3.73			Glu-88	9.03	3.62		2.00	2.13	
	7.48	3.52		3.83	4.13			8.91	3.42		1.87	2.00	
Glu-66	7.82	3.84		1.67	1.31		Lys-89	8.76	4.02		1.73	1.88	
	7.67	3.88		1.97	2.12			8.60	3.82		1.58	1.71	
Tyr-67	8.39	3.58		3.03	3.12		Asp-90	6.49	4.40		2.65	2.99	
	8.42	4.17		3.04	3.31			6.26	4.04		2.22	2.63	
Leu-68	8.32	3.07		1.22	1.77	γ 2.05, δ 0.21	Arg-91	7.59	3.93		2.21		
						δ 1.12		7.24	3.25		1.86		
	8.12	2.90		0.06	1.05	γ 0.71, δ −3.17	Asn-92	8.82	4.02		2.84	3.09	δ2 7.17, δ2 7.32
						δ −0.88		8.53	3.82		2.62	2.83	δ2 7.02, δ2 7.15
Thr-69	7.37	3.91		4.18		γ 1.10	Asp-93	8.81	4.31		2.78	2.83	
	7.42	3.82		4.32		γ 1.17		8.51	4.05		2.47		
Asn-70	6.22	4.24		2.77	2.81	δ2 6.36, δ2 7.29	Leu-94	8.66	4.35		2.03	2.24	γ 2.05, δ 1.23
	6.83	4.94		3.14	3.26	δ2 7.08, δ2 7.93							δ 1.52
Pro-71		4.27		3.22	0.83	γ 0.12, γ 0.77		8.17	3.80		1.25	1.38	γ 0.91, δ −0.08
						δ 2.77, δ 3.09							δ 0.38
		5.66		5.00		γ 2.45, γ 3.27	Ile-95	9.32	3.73		2.21		γ1 2.17, γ1 0.64
						δ 3.53, δ 4.09							γ2 0.64, δ 1.11
Tml-72[d]	7.72	3.82		1.60	1.68	$-(CH_3)_3$ 2.85		8.75	3.07		1.77		γ2 0.39, γ1 0.25
	9.43	5.21		2.63		$-(CH_3)_3$ 3.31							γ1 1.38, δ 0.54
Lys-73	7.00	4.02			1.65		Thr-96	8.29	3.93		4.53		γ 1.32
	7.88	4.55		2.05	2.15			7.98	3.72		4.27		γ 1.17
Tyr-74	7.37	4.23		3.13	3.24	δ 7.20, ϵ 6.65	Tyr-97	7.93	4.22		3.23	3.74	
	8.23	5.18		3.91	4.17	δ 7.77, ϵ 6.93		7.63	4.00		2.91	3.56	δ 5.72, δ 6.71
Ile-75	8.32	4.11			1.97	γ2 0.61							ϵ 7.16, ϵ 7.43
	9.53	4.78		3.45		γ1 1.55, γ1 3.08	Leu-98	9.42[c]	3.43		1.72	2.08	γ 2.00, δ 0.88
						γ2 1.31, δ 2.02							δ 0.95
Pro-76		4.53		1.87		γ 1.96, γ 0.61		9.04	3.26		1.28	1.87	γ 1.47, δ 0.18
						δ 3.37, δ 3.17							δ 0.70
		5.17		2.12	2.64	γ 2.33, δ 3.82	Lys-99	8.80	3.52			1.57	
Gly-77	8.68	3.62	4.25					8.58	3.38		1.27	1.45	
	9.33	3.98	4.60				Lys-100	6.61	4.22		1.43	1.83	
Thr-78	8.22	4.60		4.27		γ 0.82		6.47	4.18		1.43	1.78	
	9.03	5.18		5.78		γ 3.37	Ala-101	8.41	3.95		0.56		
Lys-79	8.77	4.44						8.38	4.03		0.68		
	8.07	4.87					Thr-102	7.45	4.37[c]				γ 0.90
Met-80	7.04	3.09		−2.43	−0.18	γ −3.72, γ −1.79		7.45	4.65				γ 1.08
						ϵ −3.19	Glu-103	6.80	4.02		2.02	2.33	
	9.70	2.72		12.94		γ −30.11, ϵ −22.82		6.90	4.05		2.05	2.37	

Heme Assignments

methyls								meso protons				
2^1	3.49	7^1	3.87	12^1	3.55	18^1	2.30	5	9.33	10	9.70	
	7.80		31.58		10.82		34.58		–		–	
thioether linkages								15	9.61	20	9.13	
3^1	5.23	3^2	1.45	8^1	6.37	8^2	2.55		0		–	
	−0.83		−2.23		2.92		2.09	17^1	4.11, 3.60	17^2	2.70, 3.37	
									–		–	

[a] Assignment in the reduced protein is given first. [b] Stereospecific assignments are not assumed. [c] These assignments were given incorrectly in Pielak et al. (1988b). They are corrected here. [d] Trimethyllysine.

three (i,i+2) NOEs over this same region indicates that this short helix is distorted. Six (i,i+2) NOEs are observed between residues 60 and 69, five of which are consecutive amide–amide (i,i+2) connectivities. Over this same region, only one (i,i+4) and three (i,i+3) connectivities are observed. We conclude that this helix also deviates from the α-helical type. Our conclusion differs from that of Feng et al. (1989). These authors did not observe α–amide (i,i+2) cross peaks and concluded that the 60s helix is a more regular α helix. [It should be pointed out that Feng et al. (1989) used a NOESY mixing time of 120 ms, compared to 133 ms used in the present study.] Between residues 70 and 74 neither (i,i+4) nor (i,i+3) connectivities are observed. However, six (i,i+2) connectivities are found, leading to the conclusion that the 70s helix is also

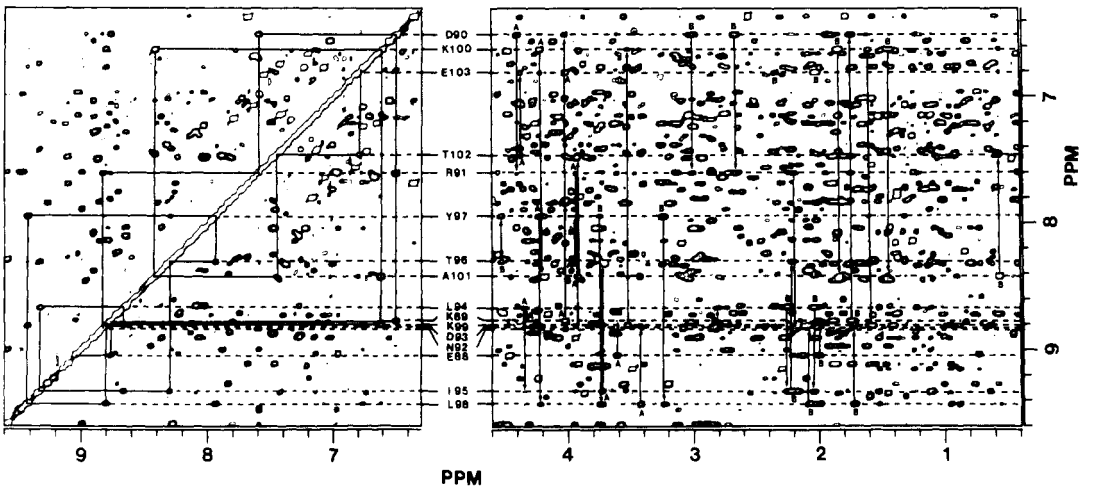

FIGURE 7: NOESY spectrum of the C102T variant of yeast iso-1-ferrocytochrome *c*. Sequential amide–amide connectivities for residues 88–103 are shown on the left; α–amide and β–amide connectivities are shown on the right. Explanation of the horizontal and vertical lines is given in the caption to Figure 6.

Table II: Backbone and β Proton Connectivities for C102T and Horse Ferrocytochrome *c*[a]

	1				5				10				15				20	
	T	E	F	K	A	G	S	A	K	K	G	A	T	L	F	K	T	R
	-	-	-	-	-		D	V	E			K	K	I		V	Q	K
d_{NH-NH}				Y	Y	Y	H	H	B	Y	B	B	B	B	B	B	B	B
$d_{\alpha-NH}$			Y	Y	Y	B	B	H		B	B	B	B	B	B	B	H	B
$d_{\beta-NH}$				Y	Y	Y	X	H	B		B	X	B	H	B	B	B	B
$d_{NH-NH}(i,i+2)$													H	H				
$d_{\alpha-NH}(i,i+2)$							Y						H	H				
$d_{\beta-NH}(i,i+2)$						X					X		H					
$d_{NH-NH}(i,i+3)$							B								Y	Y		
$d_{\alpha-NH}(i,i+3)$								H	H	B	Y	B	B		B			
$d_{\beta-NH}(i,i+3)$						X	H				X	Y	B					
$d_{\alpha-\beta}(i,i+3)$							X				Y	B	B	H		B		
$d_{\alpha-NH}(i,i+4)$											Y	Y	H					

	25				30				35				40				45	
	G	G	P	H	K	V	G	P	N	L	H	G	I	F	G	R	H	S
			K			T							L				K	T
d_{NH-NH}	B	H		B		B	X	X	B	B	B	B	B	B	H	B	Y	Y
$d_{\alpha-NH}$	B	H	H	Y	B	B	X	B	B	B	B	B	B		B	B	B	Y
$d_{\beta-NH}$	X	X	H	Y	B	B	X	B	Y	B	H	X	H	B	X	Y	B	H
$d_{NH-NH}(i,i+2)$						X		X										
$d_{\alpha-NH}(i,i+2)$						X												
$d_{\beta-NH}(i,i+2)$	X	X				X	X				X		X			X		
$d_{NH-NH}(i,i+3)$				X			X											
$d_{\alpha-NH}(i,i+3)$				X														
$d_{\beta-NH}(i,i+3)$	X	X		X		X					X		X			X		
$d_{\alpha-\beta}(i,i+3)$			X					X			X			X			X	
$d_{\alpha-NH}(i,i+4)$			X				X											

	50				55				60				65				70				75	
	D	A	N	I	K	K	N	V	L	W	D	E	N	N	M	S	E	Y	L	T	N	P
			K			G	I	T		K		E	T	L	M					E		
d_{NH-NH}	B	B	B	B	B	B	B	H		Y	B	B	B	B	B	H	B	H	B	B	X	X
$d_{\alpha-NH}$	B	B	Y	B	H	B	B	B	H	B	H	B	B	B	H	H	B	H	B	X		B
$d_{\beta-NH}$	B	B	B	B	H	B	Y	Y	Y		H	H	B	B	H	H	B	H	B	B	X	
$d_{NH-NH}(i,i+2)$			B		B						H	B	B	H	H				X	Y	B	X
$d_{\alpha-NH}(i,i+2)$				H													Y		X	B		B
$d_{\beta-NH}(i,i+2)$																			X		H	
$d_{NH-NH}(i,i+3)$											H	H										X
$d_{\alpha-NH}(i,i+3)$	B	Y										Y							X			
$d_{\beta-NH}(i,i+3)$		H	Y																	X		
$d_{\alpha-\beta}(i,i+3)$																						
$d_{\alpha-NH}(i,i+4)$	B																X				X	
$d_{NH-NH}(i,i+4)$											B						X				X	

	80				85				90				95				100			
	G	T	K	M	A	F	G	G	L	K	K	E	K	D	R	N	D	L	I	T
				I		A			I			K	T	E		E			A
d_{NH-NH}	H		B	B	B	H						B	B	B	B		Y	B	B	Y
$d_{\alpha-NH}$	H	B	H	B	B	H		B	H	H	B	B	B	B	B		Y	Y	B	B
$d_{\beta-NH}$		H	H	B	B		X	B		H	Y	B	Y	B		B	Y	B	Y	B
$d_{NH-NH}(i,i+2)$	X											B		B						Y
$d_{\alpha-NH}(i,i+2)$																			H	
$d_{\beta-NH}(i,i+2)$	X			Y				X												
$d_{NH-NH}(i,i+3)$																				
$d_{\alpha-NH}(i,i+3)$												Y	Y		Y	H	Y			
$d_{\beta-NH}(i,i+3)$	X							X												
$d_{\alpha-\beta}(i,i+3)$				X								Y				H		B	B	H
$d_{\alpha-NH}(i,i+4)$							Y													

	95				100		
	T	Y	L	K	K	A	T	E	-
								N	E
d_{NH-NH}	B	B	Y	B	B	B	B	H	X
$d_{\alpha-NH}$	B	B	Y	B	B	B	B	H	X
$d_{\beta-NH}$	B	Y	B	Y	B	B	B	H	X
$d_{NH-NH}(i,i+2)$		Y						X	X
$d_{\alpha-NH}(i,i+2)$						Y		X	X
$d_{\beta-NH}(i,i+2)$						Y		X	X
$d_{NH-NH}(i,i+3)$								X	X
$d_{\alpha-NH}(i,i+3)$								X	X
$d_{\beta-NH}(i,i+3)$								X	X
$d_{\alpha-\beta}(i,i+3)$	B	H	H	B	Y			X	X
$d_{\alpha-NH}(i,i+4)$								X	X

[a] The sequence of C102T is above the horse sequence. Only the amino acids that differ between the two proteins are shown in the horse sequence. Y, H, and B indicate that an NOE is observed in the C102T protein, the horse protein, or both proteins, respectively. X indicates that protons that might lead to this NOE are absent in both proteins. NH refers to the backbone amide protons.

irregular. Taken together, the NOE data show that the helices of the C102T variant and horse cytochrome *c* are very similar.

In the crystal structure of the yeast protein (Louie et al., 1988a) the 50s, 60s, and 70s helices are described as approximate α helices. In the low-resolution structure of the horse protein the 60s helix is described as three consecutive 3_{10} bends (Dickerson et al., 1971). The positions of these helices are between residues 49 and 56, 60 and 69, and 70 and 75 from analysis of the X-ray crystal structure and between residues 49 and 55, 60 and 69, and 71 and 75 from analysis of NOE data. It is interesting to note that α–amide $(i,i+2)$ connectivities are most usually used as evidence for a 3_{10} helix, yet we observe mostly amide–amide $(i,i+2)$ connectivities in the 60s helix.

Assignment of Exchangeable Side-Chain Proton Resonances. Exchangeable side-chain protons of Arg-13 and -38, Gln-16 and -42, Asn-31, -52, -56, -62, -63, -70, and -92, Thr-19 and -49, Tyr-46 and -48 and Trp-59 have been identified in the C102T protein (Table I). Observation of these proton resonances indicates that these side chains are buried within the protein and/or involved in hydrogen bonds to either other side chains, the backbone, or the heme propionic acids and, hence, have low mobilities. Most of these hydrogen bonds are seen in the crystal structure of rice (Ochi et al., 1983) and tuna cytochromes *c* (Takano & Dickerson, 1981a,b).

Flipping of Aromatic Side Chains. Examination of aromatic side-chain assignments for Tyr and Phe residues in the C102T variant and the horse proteins (Table I and supplementary material) indicates that there is no change in the dynamics of aromatic side chains between the two proteins as monitored by ^{1}H NMR chemical shift data. The observation of only one $\delta\backslash\epsilon$ COSY cross peak indicates that aromatic residues at positions 36, 74, and 82 are flipping rapidly (Campbell et al., 1975; Wüthrich & Wagner, 1975). Phe--3, of the N-terminal extension of the C102T variant, also exhibits rapid flipping behavior. Phe-10, Tyr-46, Tyr-48, and Tyr-97 are flipping slowly, as indicated by the observation of more than one set of $\delta\backslash\epsilon$ cross peaks. The side chain of Tyr 67 remains unassigned.

Secondary Shifts of α and Amide Protons. The secondary shift is defined as the chemical shift of a proton in the protein minus the chemical shift of the chemically equivalent proton in a random polypeptide (Bundi & Wüthrich, 1979).

Figure 8 shows the secondary shift of the reduced C102T variant. Upfield secondary shifts of about 0.5 ppm are ob-

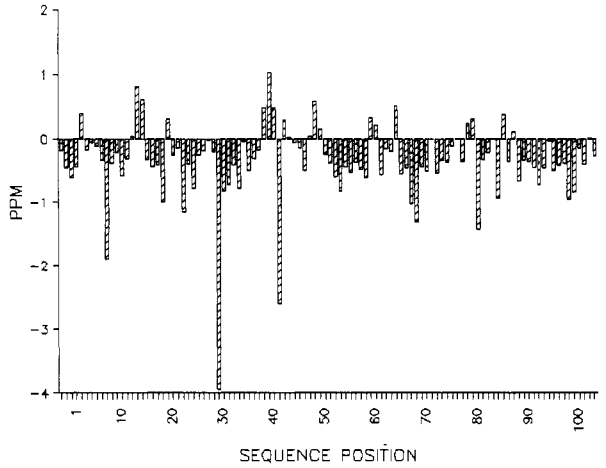

FIGURE 8: Secondary shift [chemical shift in the protein minus the shift in a random-coil polypeptide (Bundi & Wüthrich, 1975)] of the α protons of the C102T variant of yeast iso-1-ferrocytochrome *c* as a function of the primary sequence. Only the most upfield resonance of each glycine α proton was used in the calculation.

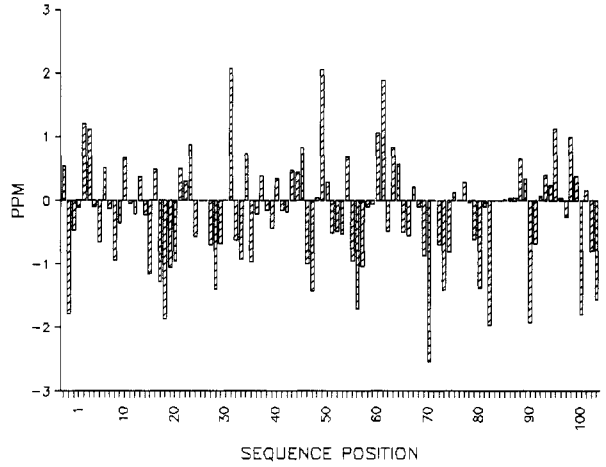

FIGURE 9: Secondary shift (as defined in Figure 8) of the amide protons of the C102T variant of yeast iso-1-ferrocytochrome *c* as a function of the primary sequence.

served for residues found in helices. This finding is in good agreement with the conclusions of Dalgarno et al. (1983) and Szilagyi and Jardetzky (1989). Upfield secondary shifts are also noted in stretches of the backbone that pass above or below the plane of the heme (residues 15–18, 20–37, 80–83). Downfield shifts are noted for residues near the heme edge (residues 12–14, 38–40, 42, 48, 47–49, 59–60). The large upfield shift observed for Gly-41 arises from the proximity of this proton to the face of the Tyr-48 aromatic ring. These observations are in accord with the diamagnetic shift calculations of Perkins (1982). These same conclusions hold for the reduced form of the horse protein and both the oxidized proteins (supplementary material).

Secondary shifts for amide protons (Figure 9 and supplementary material) are generally larger than secondary shifts for α protons, but the former do not fall so cleanly into patterns based on secondary structure or orientation of the backbone relative to the heme. Wagner et al. (1983) have previously shown that hydrogen bonds make a larger contribution to the secondary shift of amide than to α protons. It follows that small differences in hydrogen bonding between two homologous proteins can result in large changes in the secondary shift of amide protons. The influence of electric field effects, if any, has been ignored since structural changes between the two proteins appear to be too small to affect the diamagnetic

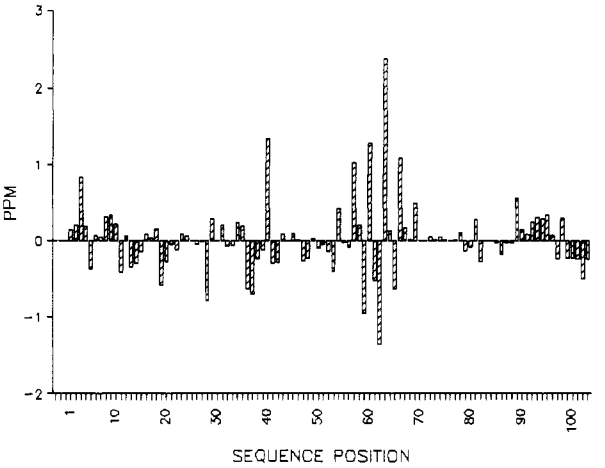

FIGURE 10: Difference in amide proton chemical shifts of the reduced C102T variant and horse cytochromes *c* as a function of the primary sequence.

shielding of amide protons. This conclusion is based on the fact that α protons, which would suffer equally from changes in diamagnetic shielding, show only very small alterations in chemical shift between the two proteins. Therefore, changes in the chemical shift of equivalent amide protons reflect changes in through-bond (i.e., hydrogen-bond) effects.

The data presented here show that upfield α proton secondary shifts are thus more diagnostic of helical secondary structure than are amide proton secondary shifts. However, *differences* in the chemical shift of amide protons between equivalent residues in homologous proteins should be diagnostic of differential backbone amide hydrogen bonding. We now go on to compare the chemical shift of the backbone protons of the two proteins.

Comparison of Amide and α Chemical Shifts between the C102T Variant and Horse Cytochrome c. As stated above, qualitative analysis of the NOE data shows that the folds of the two cytochromes *c* are very similar. The difference between the chemical shifts of the amide protons of the two ferrocytochromes *c* as a function of residue number is shown in Figure 10. These differences persist when the shifts are corrected for the amino acids which are substituted in the two proteins (data not shown). Most of the differences are less than 0.4 ppm. Larger differences are observed at residue 40, and a distinct pattern of rising and falling differences is observed between residues 53 and 70. These same patterns are observed in the oxidized form (supplementary material).

The X-ray crystal structure of yeast iso-1-cytochrome *c* and tuna cytochrome *c* indicates that a hydrogen bond is formed between the amide of residue 40 and the carbonyl oxygen of residue 57. Residue 57 is Val in the C102T variant and Ile in the horse (and tuna) protein. In their comparison of yeast iso-1-cytochrome *c* and tuna cytochrome *c*, Louie et al. (1988a) find a 1- and 2-Å difference in the position of the backbone at positions 56 and 57, respectively, due to the differential packing of the Val-57 side chain in yeast iso-1-cytochrome *c* versus the Ile-57 side chain in horse cytochrome *c* and the unique ϕ, ψ angles of Gly-56 (horse) versus Asn-56 (yeast). It seems likely that the difference in chemical shift at position 40 is due to alteration of the 40–57 hydrogen bond. The substitution at position 57 also effects the hydrogen bond formed between the amide of residue Gly-37 and the carbonyl at Trp-59.

The stretch of residues 53–70 encompasses the end of the 50s helix and the entire 60s helix. This region of the protein not only shows a distinctive pattern of chemical shift differ-

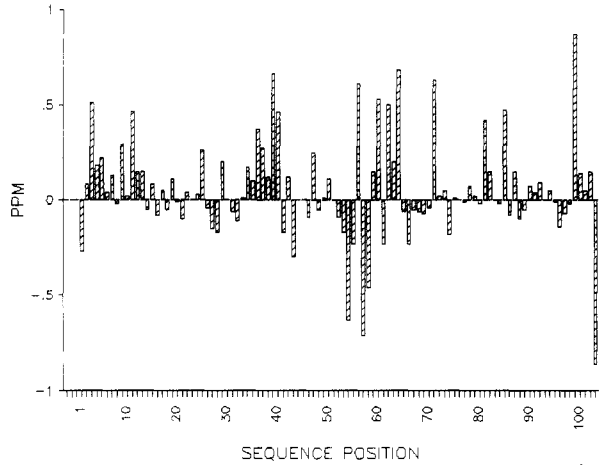

FIGURE 11: Difference in α proton chemical shifts of the reduced C102T variant and horse cytochromes *c* as a function of the primary sequence. Only the most upfield resonance of each glycine α proton was used in the calculation.

ences but also exhibits a large number of amino acid substitutions between the two proteins (Table II). In fact, this region of the cytochrome *c* family exhibits clustering of substitutions (Cutler et al., 1987) and an above average mobility as described by crystallographic *B* factors (Louie et al., 1988a). An earlier NMR study showed that this region of cytochrome *c* is flexible, and this flexibility correlates with the presence of an important antigenic determinant (Moore & Williams, 1980).

The pattern of large differences in amide chemical shift observed between the two proteins occurs in and around the 60s helix (Figure 10). There is an approximate three-residue repeat in the sign of the differences. That is, residues 59, 63, and 66 exhibit large positive differences, while residues 61, 64, 67, and 70 exhibit small differences and residues 60, 62, and 65 exhibit large negative differences. This three-residue repeat is in accord with the distorted nature of this helix as described by medium-range NOEs, discussed above. The amide protons of the hydrophobic side of the helix, facing the interior of the protein (residues 61, 64, and 67), exhibit only small differences in chemical shift between the two proteins. Gao et al. (1989) also observed only small differences at positions 61, 64, and 67 when they compared horse and tuna cytochromes *c*. Since there is no compelling evidence either from analysis of NOEs or from X-ray crystallography that there is a major change in the conformation of the 60s helix between the yeast and horse proteins, these changes in chemical shift must arise from changes in the strengths of hydrogen bonding which allows maintenance of the secondary structure in this region while accomodating changes in amino acids. The 60s helix appears to be a very malleable unit of secondary structure within cytochrome *c*. A smaller distinctive pattern of differences is observed in the C-terminal helix with a change in the sign of the chemical shift difference occurring around residue 96 (Figure 10). It is in this region that this helix crosses the plane of the heme. This pattern may be due to a slight rearrangement of the helix between the two proteins relative to the heme. This would alter the amount of heme-centered diamagnetic shift experienced by the helix, giving rise to the observed pattern of chemical shift differences. Examination of the histogram of chemical shift differences between amide protons of the oxidized C102T variant and oxidized horse cytochromes *c* (supplementary material) leads to the same conclusions for the oxidized proteins.

The difference in the chemical shift of α protons between the two reduced proteins is shown in Figure 11. The oxidized proteins exhibit the same pattern (supplementary material). The magnitudes of the average differences for α protons are significantly smaller than those for the amide protons, in agreement with the discussion on the magnitude of secondary shifts above. Although the pattern is not as clear as it is for the amide protons, clustering of large differences is evident at positions 36–40 and 55–64 and at positions 99 and 103. The differences in the first two regions are consistent with those observed for the amide protons discussed above. The large differences at positions 99 and 103 could be due to disruption of the hydrogen bond between the carbonyl oxygen of Lys-99 and the side chain of Asn-103 of horse cytochrome *c* by substitution to Glu-103 in the yeast protein.

Side-Chain Chemical Shifts and Side-Chain NOE Data. It is evident that these data can be used in detailed structural studies. It is immediately clear from our data that buried protons give NOE patterns in very clear agreement with expectations from X-ray diffraction data. In making assignments we have always checked our observations against the NOEs predicted from the crystal structure (Louie et al., 1988a). (We are extremely indebted to Professor Brayer for his assistance.) A different situation exists for surface residues, and we will turn to the analysis of NOE and other data for protons on the surface of cytochrome *c* in a subsequent paper. Here it becomes extremely important to be aware of the variability of the line width, i.e., relaxation times, and we shall need to show cross sections of the data to illustrate the problems.

Summary. NOE data presented here demonstrate conclusively that eukaryotic cytochromes *c* share a very similar fold even though many amino acid residues are not conserved between species. However, the chemical shifts of structurally equivalent (and sometimes identical) protons can vary dramatically. We have shown that chemical shift information (secondary shift and differences in chemical shift between homologous proteins) is a very sensitive measure of protein structure. Upfield secondary shifts of α protons are indicative of helical structure, while differences in backbone amide proton chemical shifts between homologous proteins are indicative of subtle changes in hydrogen bonding (or in the position of nearby dipoles) against this background. We note that there is a region of the structure which is variable.

ACKNOWLEDGMENTS

We thank Colin Greenwood and Adrian Thompson for access to and assistance in the use of their fermentation facilities and Liliana Garcia for her critical review of the manuscript. R.J.P.W. is a member of the Oxford Interdisciplinary Centre for Molecular Studies.

SUPPLEMENTARY MATERIAL AVAILABLE

Tables giving the proton assignments for reduced and oxidized horse cytochrome *c*; a table depicting the short- and medium-range backbone and β connectivities observed for the oxidized C102T variant of yeast iso-1-cytochrome *c* and oxidized horse cytochrome *c*; figures depicting portions of 2-D spectra from oxidized horse cytochrome *c*; figures depicting the difference in chemical shift between the oxidized C102T variant of yeast iso-1-cytochrome *c* and oxidized horse cytochrome *c* as a function of residue number for α protons and amide protons; figures depicting portions of the NOESY spectra of the reduced C102T variant of yeast iso-1-cytochrome *c* (51 pages). Ordering information is given on any current masthead page.

Registry No. Cytochrome *c*, 9007-43-6.

References

Bundi, A., & Wüthrich, K. (1979) *Biopolymers 18*, 285–297.

Campbell, I. D., Dobson, C. M., & Williams, R. J. P. (1975) *Proc. R. Soc. London, Ser. B 189*, 503–509.

Cutler, R. L., Pielak, G. J., Mauk, A. G., & Smith, M. (1987) *Protein Eng. 1*, 95–99.

Cutler, R. L., Davies, A. M., Creighton, S., Warshel, A., Moore, G. R., Smith, M., & Mauk, A. G. (1989) *Biochemistry 28*, 3188–3197.

Dalgarno, D. C., Levine, B. A., & Williams, R. J. P. (1983) *Bioscience Rep. 3*, 443–452.

Dickerson, R. E., Takano, T., Eisenberg, D., Kallai, O. B., Samson, L., Cooper, A., & Margoliash, E. (1970) *J. Biol. Chem. 246*, 1511–1535.

Feng, Y., Roder, H., Englander, S. W., Wand, A. J., & Di Stefano, D. L. (1989) *Biochemistry 28*, 195–203.

Gao, Y., Lee, A. D. J., Williams, R. J. P., & Williams, G. (1989) *Eur. J. Biochem. 182*, 57–65.

Hazzard, J. T., McLendon, G., Cusanovich, M. A., Das, G., Sherman, F., & Tollin, G. (1988) *Biochemistry 27*, 4445–4451.

Liang, N., Pielak, G. J., Mauk, A. G., Smith, M., & Hoffman, B. M. (1987) *Proc. Natl. Acad. Sci. U.S.A. 84*, 1249–1252.

Liang, N., Mauk, A. G., Pielak, G. J., Johnson, J. A., Smith, M., & Hoffman, B. M. (1988) *Science 240*, 311–313.

Louie, G. V., Hutcheon, W. L. B., & Brayer, G. D. (1988a) *J. Mol. Biol. 199*, 295–314.

Louie, G. V., Pielak, G. J., Smith, M., & Brayer, G. D. (1988b) *Biochemistry 27*, 7870–7876.

Matsuura, Y., Hata, Y., Yamaguchi, T., Tanaka, N., & Kakudo, M. (1979) *J. Biochem. (Tokyo) 85*, 729–737.

Moore, G. R., & Williams, R. J. P. (1980) *Eur. J. Biochem. 103*, 543–550.

Ochi, H., Hata, Y., Takana, N., Kakudo, M., Sakurai, T., Aihara, S., & Morita, Y. (1983) *J. Mol. Biol. 166*, 407–418.

Otting, G., & Wüthrich, K. (1987) *J. Magn. Reson. 75*, 546–549.

Pearce, L. L., Gärtner, A. L., Smith, M., & Mauk, A. G. (1989) *Biochemistry 28*, 3152–3156.

Perkins, S. J. (1982) *Biol. Magn. Reson. 4*, 193–336.

Pielak, G. J., Mauk, A. G., & Smith, M. (1985) *Nature (London) 313*, 152–154.

Pielak, G. J., Oikawa, K., Mauk, A. G., Smith, M., & Kay, C. M. (1986) *J. Am. Chem. Soc. 108*, 2724–2727.

Pielak, G. J., Atkinson, R. A., Boyd, J., & Williams, R. J. P. (1988a) *Eur. J. Biochem. 177*, 179–185.

Pielak, G. J., Boyd, J., Moore, G. R., & Williams, R. J. P. (1988b) *Eur. J. Biochem. 177*, 167–177.

Senn, H., Eugster, A., & Wüthrich, K. (1983) *Biochim. Biophys. Acta 743*, 58–68.

Smith, M., Leung, D. W., Gillam, S., Astell, C. R., Montgomery, D. L., & Hall, B. D. (1979) *Cell 16*, 753–761.

Sorrell, T. N., & Martin, P. K. (1989) *J. Am. Chem. Soc. 111*, 766–767.

States, D. J., Haberkorn, R. A., & Ruben, D. J. (1982) *J. Magn. Reson. 48*, 286–292.

Szilagyi, L., & Jardetzky, O. (1989) *J. Magn. Reson. 83*, 441–449.

Takano, T., & Dickerson, R. E. (1981a) *J. Mol. Biol. 153*, 79–94.

Takano, T., & Dickerson, R. E. (1981b) *J. Mol. Biol. 153*, 95–115.

Tanaka, N., Yamane, T., Tsukihara, T., Ashida, T., & Kakudo, M. (1975) *J. Biochem. (Tokyo) 77*, 147–162.

Wagner, G., Pardi, A., & Wüthrich, K. (1983) *J. Am. Chem. Soc. 105*, 5948–5949.

Wand, A. J., & Englander, S. W. (1985) *Biochemistry 24*, 5290–5294.

Wand, A. J., Di Stefano, D. L., Feng, Y., Roder, H., & Englander, S. W. (1989) *Biochemistry 28*, 186–194.

Williams, G. (1986) *J. Inorg. Biochem. 28*, 373–380.

Wüthrich, K. (1986) *NMR of Proteins and Nucleic Acids*, Wiley, New York.

Wüthrich, K., & Wagner, G. (1975) *FEBS Lett. 50*, 265–268.